

Classifier-free graph diffusion for molecular property targeting

Matteo Ninniri^{*1}, Marco Podda^{*1}, Davide Bacciu^{*1}

¹Department of Computer Science - University of Pisa
Largo Bruno Pontecorvo, 3 - 56127 Pisa (Italy)
m.ninniri1@studenti.unipi.it, marco.podda@unipi.it, davide.bacciu@unipi.it

Abstract

This work focuses on the task of property targeting: that is, generating molecules conditioned on target chemical properties to expedite candidate screening for novel drug and materials development. DiGress is a recent diffusion model for molecular graphs whose distinctive feature is allowing property targeting through classifier-based (CB) guidance. While CB guidance may work to generate molecular-like graphs, we hint at the fact that its assumptions apply poorly to the chemical domain. Based on this insight we propose a classifier-free DiGress (FreeGress), which works by directly injecting the conditioning information into the training process. CF guidance is convenient given its less stringent assumptions and since it does not require to train an auxiliary property regressor, thus halving the number of trainable parameters in the model. We empirically show that our model yields up to 79% improvement in Mean Absolute Error with respect to DiGress on property targeting tasks on QM9 and ZINC-250k benchmarks. As an additional contribution, we propose a simple yet powerful approach to improve chemical validity of generated samples, based on the observation that certain chemical properties such as molecular weight correlate with the number of atoms in molecules.

1 Introduction

The problem of generating molecules with desired chemical properties is crucial to enable fast candidate screening in the early stages of drug (Dara et al. 2021) or novel materials (Liu et al. 2017) development. Although the advent of deep learning has achieved remarkable accomplishments in computational chemistry, this strategic endeavor remains an area of active research. In the past, much of the researchers' focus has been on the task of *property optimization*, which is based on modifying an already generated molecule such that it acquires some solicited chemical property (Jin, Barzilay, and Jaakkola 2018). However, driven by the success of conditional generative models (Radford et al. 2021), an equally important – though slightly different – task has emerged recently: *property targeting*, that is, to natively generate molecules which satisfy pre-specified chemical desiderata (Sousa et al. 2021).

Among the plethora of deep generative models that have been developed in the last decade, some are based on textual representation of molecules such as SMILES (Weininger 1988) or SELFIES (Krenn et al. 2022), while others are based on generating the molecular graph directly. Regarding the latter category, which is of interest for this work, previous approaches have employed autoregressive generation conditioned on latent representations (e.g. Gómez-Bombarelli et al. 2018), as well as one-shot generation of the adjacency and node feature matrices of the molecular graph (e.g. De Cao and Kipf 2022).

Denosing Diffusion Probabilistic Models (DDPMs) (Ho, Jain, and Abbeel 2020) have been shown to achieve state-of-the-art performance in conditional generation, for example to synthesize images from user-provided textual guidance (Saharia et al. 2022). Due to their flexibility and excellent performance, DDPMs have been extended to the chemical domain and applied to with textual and graph-based approaches to tasks such as distribution learning, property optimization, and property targeting with promising results (Runcie and Mey 2023).

In particular, DiGress (Vignac et al. 2023) is one of the first successful applications of DDPMs for molecular generation. Under the hood, DiGress is based on a discrete diffusion process (Austin et al. 2021) which gradually applies noise to a molecular graph according to a transition matrix, while denoising is performed by a graph transformer network (Dwivedi and Bresson 2020). The most interesting feature of DiGress is the possibility to perform conditional generation for property targeting through classifier-based (CB) guidance (Dhariwal and Nichol 2021). Loosely speaking, CB guidance requires to train a separate classifier to predict the conditional information from noisy samples, and to inject the resulting gradients back into the reverse process to bias the generative process. While successful to some extent, CB guidance has been shown to be inherently limited by *a*) the necessity of training a separate property predictor, which defies the purpose of having a single conditional generative model in the first place, and *b*) the fact that the gradients of the property predictor are not always informative and may lead the generative process astray. Due to these limitations, in the current DDPMs practice classifier-free (CF) guidance is often preferred. The idea behind CF guidance is to directly incorporate the conditioning vector as input to train the con-

^{*}These authors contributed equally.

ditional DDPM. With respect to CB guidance, CF guidance has been shown to enable more stable training and better generative performance in general (Ho and Salimans 2022).

With DiGress, and molecular generation specifically, CB guidance is further limited by the fact that the auxiliary model is a regressor whose predictions (the chemical properties) are assumed to be normally distributed even for noisy graphs which are chemically invalid. This motivates our first contribution, which consists of the development and implementation of CF guidance for DiGress, called FreeGress. Experimentally, we show that switching from CB to CF guidance is beneficial to improve at property targeting. In particular, we evaluated FreeGress against DiGress on the QM9 (Ramakrishnan et al. 2014) and ZINC-250k (Gómez-Bombarelli et al. 2018) datasets, where we queried the models to generate molecules with properties as close as possible to a target specification. Comparing the mean absolute error between the target properties and the properties of the generated molecules, FreeGress significantly outperformed DiGress, with improvements up to 79% in the most favourable case. Besides improving performances, FreeGress does not require an auxiliary property regressor, which cuts the number of trainable parameters by half. Furthermore, guided by the observation that certain chemical properties relate to the molecular graph size (the number of atoms in the molecule), we also propose to improve the generative process by first learning the probability of sampling a certain number of nodes given the target property, and then using samples from this distribution to constrain the size of the graph to be generated. Through experiments, we show that this simple method allows to generate more chemically valid graphs without sacrificing performance.

2 Background and related works

2.1 Notation

For the purposes of this work, a molecular graph with n atoms is a tuple $G = (\mathbf{X}, \mathbf{E})$ where $\mathbf{X} \in \mathbb{R}^{n \times a}$ is a node matrix whose i -th row, indicated as $\mathbf{x}_i \in \mathbb{R}^a$, is the one-hot encoding of the atomic type of the i -th atom. Possible atomic types are specified by the set \mathcal{X} with cardinality a . Similarly, $\mathbf{E} \in \mathbb{R}^{n \times n \times b}$ is an adjacency tensor (also called edge tensor) that jointly represents the molecular connectivity and the type of bond occurring between each pair of atoms. In practice, the (i, j) -th entry of \mathbf{E} , indicated as $\mathbf{e}_{ij} \in \mathbb{R}^b$, contains the one-hot encoding of the bond type occurring between the i -th and j -th atoms. Possible bond types are specified by the set \mathcal{E} with cardinality b , where the absence of a bond is itself considered a bond type. In the following we will use the term “node” interchangeably with “atom”, and “edge” interchangeably with “bond”. Conditioning vectors will be generally represented as vectors $\mathbf{y} \in \mathbb{R}^d$, where d is usually a small integer (1 or 2 in our experiments).

2.2 Deep generative models for molecules

Historically, the first approach to use a deep generative model to produce unseen molecules has been proposed by Gómez-Bombarelli et al. (2018). Essentially, the model is a

VAE where both the encoder and decoder are recurrent neural networks trained to reconstruct SMILES strings. In particular, the decoder is essentially an autoregressive SMILES language model capable of generating a molecule by sampling one SMILES character at a time. Although simplistic, this model still remains one of the most efficient. The model was designed to allow property optimization through Bayesian optimization in latent space. Over the years, several variants to address limitations such as low validity rates (Kusner, Paige, and Hernández-Lobato 2017) or the inability to handle more complex chemical substructures at the vocabulary level (Podda, Bacciu, and Micheli 2020) have been developed. Other methods related to this generative flavour use the alternative language of SELFIES instead, which is deemed to be more robust than SMILES as every possible character sequence defines a valid molecule. A different branch of methods is focused on generating the molecular graph directly. In this case, two possibilities have been explored: generating the graph autoregressively – either atom-by-atom (Li et al. 2018), edge-by-edge (You et al. 2018b; Goyal, Jain, and Ranu 2020; Bacciu and Podda 2021), or motif-by-motif (Jin, Barzilay, and Jaakkola 2020) – or directly predicting the adjacency and node feature matrices (De Cao and Kipf 2022). On graph-based models, property optimization has been performed with simple hill climbing in latent space (guided by a property predictor), up to iterative reinforcement learning approaches which assign higher rewards to chemically appealing molecules (You et al. 2018a). In particular, Jin, Barzilay, and Jaakkola (2020) propose to cast the property optimization problem as a molecular translation problem, where the difference between two molecules (one with suitable chemical properties, the other chemically similar but with poor chemical properties) is mapped to a Gaussian manifold. Latent vectors sampled from this prior can be used to modify unsuitable molecules into suitable ones. Lately, DDPMs that generate the molecular graph have started to be used for distribution learning as well as property optimization tasks. The primary application of DDPMs is 3D structure generation, which is useful to handle a different class of tasks such as ligand generation conditioned on the coordinates of a protein pocket (Baillif et al. 2023). Among DDPM-based models, DiGress was the first to be applied to 2D molecule generation, as well as one of the first to formalize the property targeting task.

2.3 DiGress: Denoising Diffusion for Graphs

Here we briefly describe DiGress (Vignac et al. 2023), a discrete DDPM for graphs which is the starting point of this study. Preliminarily, we provide a brief introduction to DDPM to set the notation and concepts for understanding our contribution.

Denoising Diffusion Probabilistic Models. DDPMs consist of an untrained *forward process* $q(\mathbf{x}^t | \mathbf{x}^{t-1})$ paired with a parameterized *reverse process* $p_\theta(\mathbf{x}^{t-1} | \mathbf{x}^t)$. The former iteratively perturbs the initial data point \mathbf{x}^0 to transform it into an \mathbf{x}^T which is akin to Gaussian noise, while the second is trained to incrementally remove the noise from \mathbf{x}^T until \mathbf{x}^0 is restored. Data generation from a trained DDPM

is performed by sampling noise $\tilde{\mathbf{x}}^T \sim \mathcal{N}(0, \mathbf{I})$, where \mathcal{N} is an isotropic Gaussian, and iteratively applying the denoising model for T steps until a new datapoint $\tilde{\mathbf{x}}^0 \sim q$ is obtained.

Conditioned generation in DDPMs is achieved by injecting a *guidance vector*, or *guide* \mathbf{y} , to obtain a *conditioned reverse process* $p_\theta(\mathbf{x}^{t-1}|\mathbf{x}^t, \mathbf{y})$. CB guidance (Dhariwal and Nichol 2021) refactors the reverse process as $p_\theta(\mathbf{x}^{t-1}|\mathbf{x}^t)p_\phi(\mathbf{y}|\mathbf{x}^{t-1})$, where $p_\phi(\mathbf{y}|\mathbf{x}^{t-1})$ is an auxiliary classifier trained to predict the guide from a noisy version of the input. A scaled version of the gradient $\nabla_{\mathbf{x}^t}$ of g_ϕ is then added to the denoising gradient in order to magnify the conditioning signal. CB guidance is limited by the fact that it requires to train the auxiliary classifier, without the possibility of exploiting pre-trained models; moreover, since only few parts of the noisy \mathbf{x}^t are actually useful to predict \mathbf{y} , the resulting gradient could yield undesirable directions in input space. In contrast, CF guidance (Ho and Salimans 2022) works by jointly optimizing $p_\theta(\mathbf{x}^{t-1}|\mathbf{x}^t, \mathbf{y})$, the conditioned model, and $p_\theta(\mathbf{x}^{t-1}|\mathbf{x}^t)$, the unconditioned model, at the same time. During sampling, the reverse process is computed as $(1+w)p_\theta(\mathbf{x}^{t-1}|\mathbf{x}^t, \mathbf{y}) - wp_\theta(\mathbf{x}^{t-1}|\mathbf{x}^t)$, which is a barycentric combination between the conditioned and unconditioned predictions with weight $w \in \mathbb{R}_+$.

DDPMs defined as above are not suited for discrete data such as graphs, since discrete distributions cannot be effectively corrupted using Gaussian noise. Instead, discrete DDPMs (Austin et al. 2021), including DiGress, inject noise in the data at time-step $t-1$ by multiplying it against a *transition matrix* \mathbf{Q}^t , where $[\mathbf{Q}^t]_{ij} = q(x^t = j|x^{t-1} = i)$, which loosely speaking specifies the probability of changing \mathbf{x} from category i to category j .

DiGress Forward process. DiGress applies noise to a molecular graph G at time-step t according to the following process:

$$q(G^t|G^{t-1}) = (\mathbf{X}^{t-1}\mathbf{Q}_X^t, \mathbf{E}^{t-1}\mathbf{Q}_E^t), \quad (1)$$

where \mathbf{Q}_X^t and \mathbf{Q}_E^t are transition matrices applied to the node matrix and the edge tensor, respectively. In particular, \mathbf{Q}_X^t is chosen from the following distribution:

$$\mathbf{Q}_X^t = \alpha^t \mathbf{I} + \beta^t \mathbf{1}_a \mathbf{m}_X, \quad (2)$$

where \mathbf{m}_X is a vector containing the marginal distribution of the node types in the training set, α^t is a noise scheduler, and $\beta^t = 1 - \alpha^t$. In practice, the transition probability to a certain node type is given by its frequency in the training set. The transition tensor \mathbf{Q}_E^t is chosen analogously. Unrolling the forward process equation, we can sample G^t given G^0 in a single step as follows:

$$q(G^t|G^0) = (\mathbf{X}\bar{\mathbf{Q}}_X^t, \mathbf{E}\bar{\mathbf{Q}}_E^t), \quad (3)$$

where $\bar{\mathbf{Q}}_X^t = \bar{\alpha}^t \mathbf{I} + \bar{\beta}^t \mathbf{1}_a \mathbf{m}_X$, $\bar{\alpha}^t = \prod_{\tau=1}^t \alpha^\tau$, and $\bar{\beta}^t = 1 - \bar{\alpha}^t$. Notice that $\bar{\mathbf{Q}}_E^t$ is defined analogously.

DiGress Reverse process. DiGress reconstructs a molecular graph from a noisy sample with the following reverse process:

$$p_\theta(G^{t-1}|G^t), \quad (4)$$

which can be thought of as the joint distribution of the individual nodes and edges given the current graph. By assuming independence, we can rewrite the joint as a product of conditionals:

$$\prod_{1 \leq i \leq n} p_\theta(\mathbf{x}_i^{t-1}|G^t) \prod_{1 \leq i, j \leq n} p_\theta(\mathbf{e}_{ij}^{t-1}|G^t). \quad (5)$$

In turn, each node conditional is computed by marginalizing over the node types (resp. edge types for the edge conditionals). Specifically, we have:

$$p_\theta(\mathbf{x}_i^{t-1}|G^t) = \sum_{\mathbf{x} \in \mathcal{X}} q(\mathbf{x}_i^{t-1}|\mathbf{x}_i^t, \mathbf{x}_i^0 = \mathbf{x}) f_\theta(\mathbf{x}_i^0 = \mathbf{x}|G^t), \quad (6)$$

where f_θ is computed by a neural network trained to infer the node types of the true graph G^0 from a noisy version G^t . The edges marginal is computed similarly, by predicting the true edge types from their noisy intermediates. CB guidance for DiGress is achieved by specifying the conditioned reverse process as:

$$p_\theta(G^{t-1}|G^t)p_\phi(\mathbf{y}|G^{t-1}), \quad (7)$$

where $p_\phi(\mathbf{y}|G^{t-1}) \propto \exp(-\lambda \langle \nabla_{G^t} \|\mathbf{y} - g_\phi(G^t)\|^2, G^{t-1} \rangle)$, g_ϕ is an auxiliary property regressor, and λ is a hyperparameter that magnifies the conditioning gradient.

Limitations. While the development of unconditioned DiGress appears intuitive, the use of CB guidance for the conditional variant leads to design choices and assumptions that are unrealistic in the chemical domain. Firstly, CB guidance relies on an external predictor that learns chemical properties from noisy graphs, which implies that chemically invalid molecules are unnaturally related to valid ones by being assigned the same properties. Secondly, the distribution learned by the auxiliary property regressor is assumed to be Normal with mean $p(\mathbf{y}|G^t)$, approximated by g_ϕ by minimizing a mean squared error objective. This assumption is unsupported by premise for most denoising steps (where G^t usually represents an invalid molecule), since it implies a distribution of chemical properties for an object that does not even exist in chemical space. Moreover, even if two molecules with graphs G^t and G^{t-1} are both valid and similar, their chemical properties can be drastically different, since molecular property landscapes are in general non-smooth (Aldeghi et al. 2022), violating again the normality assumption. This discussion motivates our intention to develop CF guidance for DiGress with the objective of making the conditional process simpler and at the same time appropriate for the chemical context where it is applied.

3 Classifier-Free Graph Diffusion Process

In this section, we first work out how to incorporate CF guidance into the general architecture of DiGress. Then, we detail the specifics of the neural architecture implementing CF guidance. Finally, we describe a chemically-motivated variant of our approach based on predicting the number of nodes of the graph to be generated from the conditioning vector.

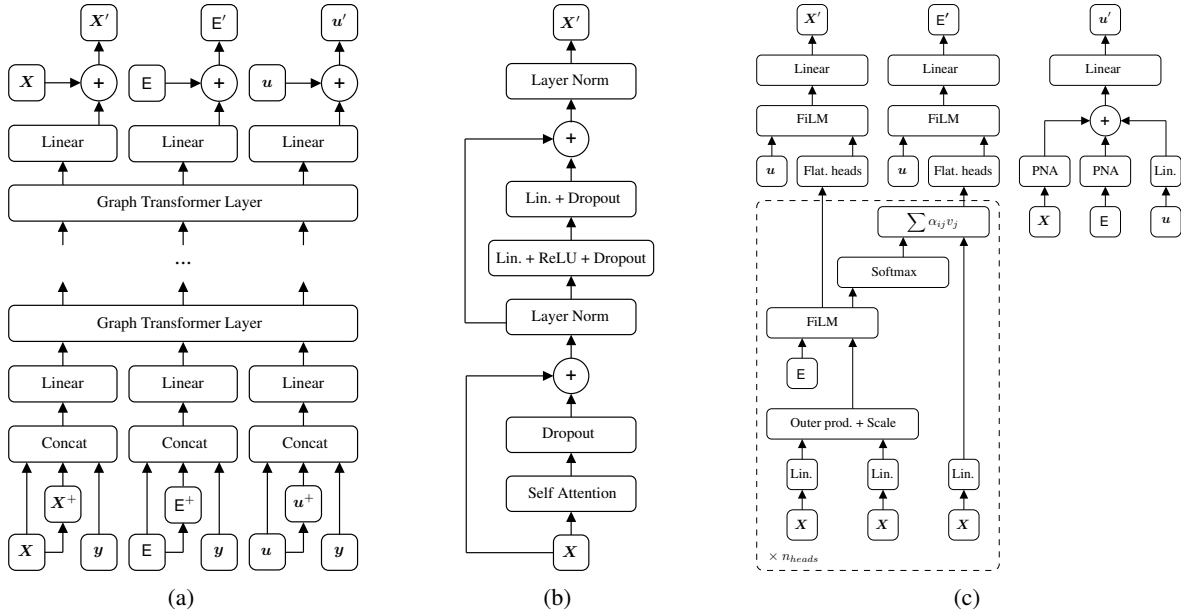


Figure 1: (a) The overall architecture of the proposed Neural Network. Notice that the guide y is now an input to the model. (b) The graph transformer layer for the input X (it is applied analogously to E and u). (c) The self attention layer within the graph transformer layer. Notice that we superimposed ' to the vectors indicate that they are network/layer outputs.

3.1 Classifier-free DiGress (FreeGress)

The forward noise process for our CF method can be straightforwardly inherited by discrete DDPM in general, and for the sake of this work from DiGress, as detailed in (1) and (2). The key impact of CF guidance is instead on the adaptive reverse process. To this end, we begin by rewriting the conditioned reverse process $p_\theta(G^{t-1}|G^t, y)$ to incorporate y as follows:

$$\prod_{1 \leq i \leq n} p_\theta(x_i^{t-1}|G^t, y) \prod_{1 \leq i, j \leq n} p_\theta(e_{ij}^{t-1}|G^t, y), \quad (8)$$

which requires to reformulate the marginals from Eq. 6. Specifically, we can rewrite the nodes marginal along the lines of Gu et al. (2022) as:

$$\sum_{x \in \mathcal{X}} q(x_i^{t-1}|x_i^t, x_i^0 = x) f_\theta(x_i^0 = x|G^t, y), \quad (9)$$

where f_θ is a neural network that predicts the true node types x^0 using both the current noisy graph G^t and the guide y . Similarly, the edges marginal is expressed as:

$$\sum_{e \in \mathcal{E}} q(e_{ij}^{t-1}|e_{ij}^t, e_{ij}^0 = e) f_\theta(e_{ij}^0 = e|G^t, y). \quad (10)$$

At this point, we have, in principle, a classifier-free DDPM. However, conditioning might not work as expected in this scenario, since the model could learn to completely ignore the guide y . To prevent this undesirable behaviour, we leverage *conditional dropout* (Ho and Salimans 2022), where the conditioning vector y is replaced, with probability p_{uncond} , by a non-parametrized placeholder \bar{y} . To summarize, the final vector y employed in the equations (and,

consequently, in the neural network) is chosen as follows:

$$y \leftarrow \begin{cases} \bar{y} & \text{with probability } p_{uncond} \\ y & \text{with probability } 1 - p_{uncond} \end{cases} \quad (11)$$

Intuitively, the placeholder signals the network to perform inference without guidance vector, as if the process was unconditioned. As a result, the model becomes capable of performing both conditioned and unconditioned sampling.

The major difference between (Ho and Salimans 2022) and our work is the fact that the former is designed for continuous signals, such as images, and their neural network is trained to predict the Gaussian noise ϵ corrupting the input signal x^t given both the latter and the conditioning vector y . FreeGress, instead, is designed for discrete graphs and its neural network is trained to infer G^0 given the corrupted graph G^t and conditioning vector y . To complete derivation of FreeGress, we build on Tang et al. (2023) and express f_θ as:

$$f_\theta(x_i^0 = x|G^t, y) = p_\theta(x_i^0|G^t, y) p_\theta(y|x_i^0, G^t)^s, \quad (12)$$

where the first term is the standard reverse process, and the second forces the model to take the guide into account, with $s \in \mathbb{R}_+$ being its relative importance. This same objective can be expressed in log-probability space as:

$$\log p_\theta(x_i^0|G^t) + (s + 1) \log p_\theta(y|x_i^0, G^t). \quad (13)$$

Lastly, using Bayes' rule, the term $\log p_\theta(y|x_i^0, G^t)$ is decomposed as:

$$\log p_\theta(x_i^0|G^t, y) - \log p_\theta(x_i^0|G^t), \quad (14)$$

which is computable since the model can output the unconditioned probability using the placeholder in place of the

guide or, more formally, since $p(\mathbf{x}_i^0|G^t) \approx p_\theta(\mathbf{x}_i^0|G^t, \bar{\mathbf{y}})$. The process is symmetric for the edges $e \in \mathcal{E}$. Finally, to add more flexibility, we parametrize $\bar{\mathbf{y}}$ so that it is learned along with the parameters θ .

Neural Architecture In order to accommodate the explicit guidance, we modified the original DiGress architecture as shown in Figure 1a. Basically, the network consists of a stack of Graph Transformer layers. In its original implementation, DiGress allows to augment the input matrices \mathbf{X} and \mathbf{E} with arbitrary node and edge features deemed useful (indicated with the + superscript in Figure 1a). In addition, a vector \mathbf{u} containing the current time step t is added, which itself be enriched with graph-wise features. All these data are augmented with the guide \mathbf{y} and processed by the stack of graph transformer layers. The graph transformer is displayed in Figure 1b: at a high level, it resembles a standard transformer architecture, with a self attention module followed by dropout, residual connection, layer norm, and a feedforward stack. The self attention layer (shown in Figure 1c) first processes the (augmented) \mathbf{X} matrix through the standard outer product and scaling typical of attention layers. Then, the result is used in conjunction with the edge tensor \mathbf{E} as input to a FiLM layer (Perez et al. 2018) to produce unnormalized attention scores. The scores are passed through a softmax layer, combined once again with the values \mathbf{X} . The attention vectors are then flattened and mixed with the vector \mathbf{u} through another FiLM layer, and then transformed linearly to obtain the prediction logits. The vector \mathbf{u} is instead processed differently, as shown visually in the rightmost part of Figure 1c. Specifically, \mathbf{X} and \mathbf{E} are first passed through independent PNA layers (Corso et al. 2020) and then summed together with a linear projection of \mathbf{u} to form the final representation.

Loss function. During training, FreeGress optimizes the following loss function for a given time step t :

$$\delta \sum_{1 \leq i \leq n} \text{NLL}(\mathbf{x}_i^0, f_\theta(\mathbf{x}_i^t)) + \gamma \sum_{1 \leq i, j \leq n} \text{NLL}(\mathbf{e}_{ij}^0, f_\theta(\mathbf{e}_{ij}^t)),$$

which is the negative log-likelihood (NLL) between the actual node (resp. edge) types and those predicted by the neural network described above. Parameters δ and γ adjust the preference towards nodes or edges prediction.

Conditioned Inference At each reverse process iteration, FreeGress generates a slightly denoised graph by first computing from the network $\log p_\theta(\mathbf{x}_i^0|\mathbf{x}_i^t, \mathbf{y})$, the conditioned log probability, and $\log p_\theta(\mathbf{x}_i^0|\mathbf{x}_i^t, \bar{\mathbf{y}})$, the unconditioned one. The final probability is obtained by exponentiating the sum of the two terms while giving an arbitrary (usually larger) weight s to the conditioned probability:

$$\log p(\mathbf{x}_i^0|G^t) + (s + 1) (\log p(\mathbf{x}_i^0|G^t, \mathbf{y}) - \log p(\mathbf{x}_i^0|G^t)),$$

where we omit exponentiation for conciseness, which corresponds to $f_\theta(\mathbf{x}^0 = \mathbf{x}|G^t, \mathbf{y})$ in Eq. 12. Then, the posteriors $q(\mathbf{x}_i^{t-1}|\mathbf{x}_i^t, \mathbf{x}_i^0 = \mathbf{x})$ are computed $\forall \mathbf{x} \in \mathcal{X}$ and summed as in Eq. 9. This procedure is executed for each atom in the graph, and the resulting probabilities are sampled to obtain the nodes of the graph G^{t-1} . The process is symmetric for the graph edges.

3.2 Graph size inference

One limitation of diffusion models as a whole is the fact that the size (for graphs specifically, the number of nodes) of a sample cannot change during the denoising process. Some studies consider the possibility of inserting and removing elements from a generated, mono-dimensional sequence (Johnson et al. 2021) but, to the best of our knowledge, there are no similar works for graphs. In the original implementation of DiGress, the number of nodes the generated graph will have is sampled from the marginal distribution computed from the training and validation sets, respectively. While this is not an issue for unconditioned sampling, we observed that for conditioned sampling, a certain property (e.g. molecular weight) might be featured only by molecules with a specific number of atoms. To solve this problem, we propose that the number of nodes n of the graph to be generated is sampled from $p_\varepsilon(n|\mathbf{y})$, which is parametrized as a neural network with two hidden layers and a softmax output layer. Here, the idea is to exploit the guide even before generation starts, by providing a graph size which is correlated with the requested property.

4 Experiments

Here, we detail the experimental analysis to evaluate FreeGress on property targeting tasks, that is, generating compounds which meet pre-specified molecular properties.

4.1 Dataset

Our experiments were conducted on QM9, a dataset of 133k small molecules (up to 9 heavy atoms) which was also part of the evaluation of DiGress, and ZINC-250k, a collection of 250k drug-like molecules selected from the ZINC dataset. For the latter, the molecules were first preprocessed by removing non-neutral charges and stereochemistry information, reducing the dataset size to 204k molecules.

4.2 Metrics and targets

All the experiments were performed using the following scheme. After we trained each model, we randomly sampled 100 molecules from the dataset and computed the desired target properties as vectors \mathbf{y} , which were used as conditioning vectors. Then, we used the vectors 10 times each to perform conditioned generation, for a total of 1000 generated molecules for each model. We computed the desired properties on the generated samples¹ and compared the results with the properties of the original samples. The metric chosen for the comparison is the Mean Absolute Error (MAE) between the target properties and the properties of the generated molecules:

$$\frac{1}{1000} \sum_{i=1}^{100} \sum_{j=1}^{10} |\mathbf{y}_i - \hat{\mathbf{y}}_{i,j}|,$$

where \mathbf{y}_i are the target properties of the i -th molecule from the dataset and $\hat{\mathbf{y}}_{i,j}$ is the target property of the j -th molecule

¹Using packages such as RDKit (Landrum 2016) and psi4 (Turney et al. 2012)

generated using the properties of the i -th molecule as guide. The targeted properties were dipole moment μ and the Highest Occupied Molecular Orbital (HOMO) for QM9; for ZINC-250k, we targeted log-partition coefficient (LogP) and Molecular Weight (MW).

4.3 Experimental details

QM9. On QM9, we trained a set of FreeGress variants against the published results of DiGress. In the original article, DiGress was trained for the property targeting task without additional features, and hyper-parameters such as λ (which regulates the impact of the regressor’s gradient) were not provided. FreeGress instances were trained with $s = 5$, and with $p_{uncond} = \{0, 0.1, 0.2\}$ to study the effect of conditional dropout on the generative process. Moreover, we also trained different variants with and without additional features for \mathbf{X} and \mathbf{u} , to understand if they provided any positive impact. Additional graph-wise features considered for this study were number of k -cycles with $k \in \{1, \dots, 6\}$, number of connected components, first 5 non-zero eigenvalues, molecular weight; among node-wise features, we considered the atom’s valency, the number of k -cycles a node belongs to, and an estimation of the biggest connected component size. FreeGress used similar hyper-parameters (5 graph transformer layers; embedding size of 256 for \mathbf{X} and 128 for both \mathbf{E} and \mathbf{u} ; 8 attention heads; $T = 500$, 1200 training epochs with batch size 512; Amsgrad optimizer (Reddi, Kale, and Kumar 2018) with learning rate of 2^{-4} and weight decay of 1^{-12} ; $\gamma = 2\delta$) as DiGress for a fair comparison. Importantly, since FreeGress does not require an auxiliary regressor, all the variants are trained with half the number of parameters than DiGress (4.6 million vs. 9.2 million, approximately). All models required approximately seven hours to train on a nVidia A100 with 80GB of VRAM.

ZINC-250k. For this dataset, we used a slightly different experimental setup since DiGress was not evaluated on this dataset previously. Specifically, we trained from scratch both DiGress and FreeGress with 12 layers and 1000 training epochs with batch size 256, while keeping the other hyper-parameters the same as for QM9. We used larger models since ZINC-250k includes bigger (in terms of number of atoms) and more diverse molecules. Training required approximately 100 hours for 1000 epochs each on the same machine as above. While FreeGress variants used approximately 16 million parameters, DiGress used approximately 32 million including the property regressor. We trained without additional features, since preliminary experiments have revealed that they had little to no influence on the performance, while at the same time largely increasing the training time. For DiGress, we evaluated different variants alternatives with $\lambda = \{50, 500, 1000, 3000\}$. For FreeGress, we fixed $s = 2$ and $p_{uncond} = 0.1$ and evaluated one variant with the inference method proposed in Section 3.2, and one without. In the former case, $p_\varepsilon(n|\mathbf{y})$ was parameterized as a neural network with 2 layers with 512 units each, and ReLU activations.

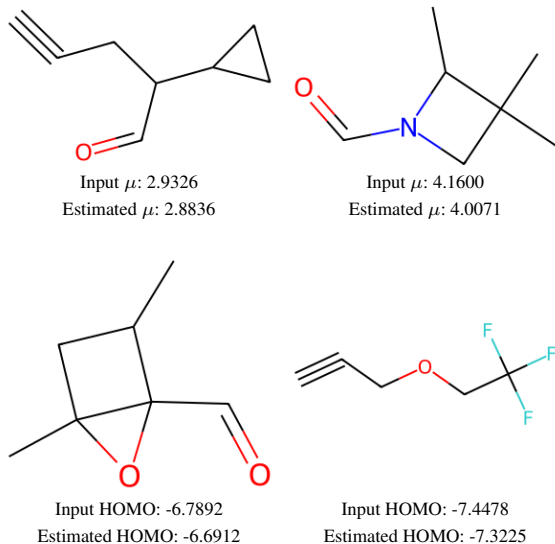


Figure 2: Curated molecules from the QM9 dataset.

5 Results

The experimental results are presented in Table 1. Novelty and uniqueness scores are not reported as they approached 100% in almost all cases. On the QM9 dataset (top table), we observe that FreeGress outperforms DiGress in almost every variant tested. Interestingly enough, even variants of FreeGress with $p_{uncond} = 0$, i.e. those that use the guide without conditional dropout, achieve comparable performance with DiGress, with the only exception of the dipole moment μ . Overall, the best performing variant of FreeGress ($p_{uncond} = 0.1$, $s = 5$, additional features) improves with respect of DiGress by 50% on the HOMO task, by 33% on the μ task, and by 39% on the combination of both. Similar improvements are achieved with slightly different combinations of the hyper-parameters, showing that CF guidance is robustly a better alternative to CB guidance for conditioned generation. Also, one should take into account that CF guidance does not require to train a separate auxiliary regressor, which saves up computational and memory resources. Four conditioned samples (two for each property targeting task) generated from the QM9 dataset are shown in Figure 2.

The analysis of performance in the ZINC-250k provides some additional interesting insights. Firstly, we observe a drop in validity of DiGress whenever too much weight is put on the auxiliary regressor by increasing λ . This is a clear signal that the gradient of the regressor is not providing useful directions in chemical space, which validates our belief that CB guidance, as formulated in DiGress, is based on unrealistic assumptions for the chemical domain. Secondly, we observe that FreeGress outperforms again DiGress on the two tasks by a great margin. Specifically, on the LogP task, FreeGress achieves a 69% improvement in MAE with respect to the best DiGress variant, while at the same time

Model	Hyper-parameters	Extra features	HOMO ↓	μ ↓	HOMO + μ ↓
DiGress	Not provided	No	0.56 ± 0.01	0.81 ± 0.04	0.87 ± 0.03
FreeGress	$p_{uncond} = 0, s = 5$	No	0.50 ± 0.05	0.99 ± 0.08	0.74 ± 0.06
	$p_{uncond} = 0, s = 5$	Yes	0.34 ± 0.03	0.95 ± 0.07	0.62 ± 0.04
	$p_{uncond} = 0.1, s = 5$	No	0.30 ± 0.04	0.60 ± 0.06	0.59 ± 0.07
	$p_{uncond} = 0.1, s = 5$	Yes	0.28 ± 0.04	0.54 ± 0.06	0.53 ± 0.07
	$p_{uncond} = 0.2, s = 5$	No	0.31 ± 0.05	0.64 ± 0.07	0.62 ± 0.06
	$p_{uncond} = 0.2, s = 5$	Yes	0.36 ± 0.10	0.57 ± 0.07	0.55 ± 0.06

Model	Hyper-parameters	LogP		MW	
		MAE ↓	Valid ↑	MAE ↓	Valid ↑
DiGress	$\lambda = 50$	1.15 ± 0.09	75%	73.40 ± 7.10	75%
	$\lambda = 500$	0.60 ± 0.05	68%	60.30 ± 6.10	73%
	$\lambda = 1000$	0.49 ± 0.05	65%	61.10 ± 5.90	69%
	$\lambda = 3000$	0.52 ± 0.13	39%	64.10 ± 5.90	59%
FreeGress	$p_{uncond} = 0.1, s = 2$	0.15 ± 0.02	85%	15.73 ± 2.74	58%
	$p_{uncond} = 0.1, s = 2, NI$	0.16 ± 0.01	84%	15.18 ± 2.71	75%

Table 1: Results on the QM9 (top) and ZINC-250k (bottom) datasets. Property targeting has been evaluated using Mean Absolute Error (see Section 4.2). HOMO: Highest Occupied Molecular Orbital; μ : dipole moment; λ : weight of the classier gradient for CB guidance; s : weight of conditioned inference for FreeGress; p_{uncond} : conditional dropout parameter for FreeGress; Valid: percentage of valid molecules among those sampled; NI: node inference (see Section 3.2).

improving validity by 31%. On the MW task, the improvement in MAE is of about 79% with respect to the best DiGress variant. Thirdly, we observe that node inference has not a decisive impact in the LogP task. However, in the MW task, it improves the validity rate from 58% to 75% (on par with the best DiGress variant), while also slightly improving in terms of MAE. This aligns with our intuition: in fact, molecules with higher molecular weight are in general more likely to have more atoms than molecules with lower molecular weight. Thus, it makes sense, in this particular task, to having a mechanism to infer the number of nodes from the guide to bias the sampling process. Figure 2 shows 4 exemplar molecules (2 for each task) generated from the ZINC-250k dataset.

6 Conclusions

This work has developed and implemented FreeGress, a discrete DDPM for graphs with CF guidance, which allows to generate molecules complying to a pre-specified set of desired chemical properties. Through experiments, we have shown that CF guidance allows to generate better (more tailored to the specification) molecules than CB guidance without sacrificing chemical validity. Of course, there are still limitations to overcome, which we intend to address in future studies: for example, even if CF guidance allows to achieve good validity rates, the model is still far from achieving perfect validity. This might be addressed by designing the forward and reverse processes to use conditional transition matrices. Another way to increase the percentage of valid molecules generated without overfitting may be to train a model to work with molecular fragments instead of atoms, as it would likely reduce the amount of points in the molecular graph where an illegal structure is generated. We also have shown that inferring the number of nodes from the

guide might be of help to generate graphs in some settings, especially when there is reason to believe that the guide is correlated with the graph’s size. As future work, we intend to validate this finding also in the more general setting of arbitrary graph generation.

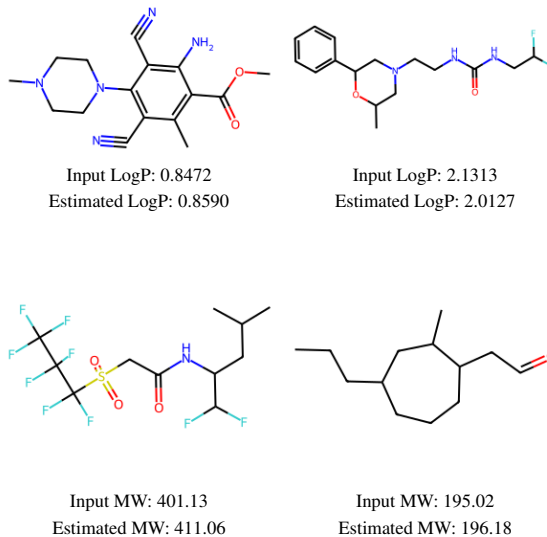


Figure 3: Curated molecules from the ZINC-250k dataset.

References

Aldeghi, M.; Graff, D. E.; Frey, N.; et al. 2022. Roughness of Molecular Property Landscapes and Its Impact on

- Modellability. *Journal of Chemical Information and Modeling*, 62(19): 4660–4671.
- Austin, J.; Johnson, D. D.; Ho, J.; Tarlow, D.; and van den Berg, R. 2021. Structured Denoising Diffusion Models in Discrete State-Spaces. In *Advances in Neural Information Processing Systems*, volume 34, 17981–17993. Curran Associates, Inc.
- Bacciu, D.; and Podda, M. 2021. GraphGen-Redux: A Fast and Lightweight Recurrent Model for labeled Graph Generation. In *2021 International Joint Conference on Neural Networks (IJCNN)*, 1–8. IEEE.
- Baillif, B.; Cole, J.; McCabe, P.; et al. 2023. Deep generative models for 3D molecular structure. *Current Opinion in Structural Biology*, 80.
- Corso, G.; Cavalleri, L.; Beaini, D.; et al. 2020. Principal Neighbourhood Aggregation for Graph Nets. In *Advances in Neural Information Processing Systems*, volume 33. Curran Associates, Inc.
- Dara, S.; Dhamecherla, S.; Jadav, S. S.; et al. 2021. Machine Learning in Drug Discovery: A Review. *Artificial Intelligence Review*, 55(3): 1947–1999.
- De Cao, N.; and Kipf, T. 2022. MolGAN: An implicit generative model for small molecular graphs. arXiv:1805.11973.
- Dhariwal, P.; and Nichol, A. 2021. Diffusion Models Beat GANs on Image Synthesis. In *Advances in Neural Information Processing Systems*, volume 34, 8780–8794. Curran Associates, Inc.
- Dwivedi, V. P.; and Bresson, X. 2020. A Generalization of Transformer Networks to Graphs. *ArXiv*, abs/2012.09699.
- Goyal, N.; Jain, H. V.; and Ranu, S. 2020. GraphGen: A Scalable Approach to Domain-Agnostic Labeled Graph Generation. In *Proceedings of The Web Conference 2020*, 1253–1263. New York, NY, USA: Association for Computing Machinery. ISBN 9781450370233.
- Gu, S.; Chen, D.; Bao, J.; et al. 2022. Vector Quantized Diffusion Model for Text-to-Image Synthesis. arXiv:2111.14822.
- Gómez-Bombarelli, R.; Wei, J. N.; Duvenaud, D.; et al. 2018. Automatic Chemical Design Using a Data-Driven Continuous Representation of Molecules. *ACS Central Science*, 4(2): 268–276.
- Ho, J.; Jain, A.; and Abbeel, P. 2020. Denoising Diffusion Probabilistic Models. In *Advances in Neural Information Processing Systems*, volume 33, 6840–6851. Curran Associates, Inc.
- Ho, J.; and Salimans, T. 2022. Classifier-Free Diffusion Guidance. In *NeurIPS 2021 Workshop DGMs Applications*.
- Jin, W.; Barzilay, D.; and Jaakkola, T. 2020. Hierarchical Generation of Molecular Graphs using Structural Motifs. In *Proceedings of the 37th International Conference on Machine Learning*, volume 119 of *Proceedings of Machine Learning Research*, 4839–4848. PMLR.
- Jin, W.; Barzilay, R.; and Jaakkola, T. 2018. Junction Tree Variational Autoencoder for Molecular Graph Generation. In *Proceedings of the 35th International Conference on Machine Learning*, volume 80 of *Proceedings of Machine Learning Research*, 2323–2332. PMLR.
- Johnson, D. D.; Austin, J.; van den Berg, R.; et al. 2021. Beyond In-Place Corruption: Insertion and Deletion In Denoising Probabilistic Models. In *ICML 2021 Workshop INN*.
- Krenn, M.; Ai, Q.; Barthel, S.; et al. 2022. SELFIES and the future of molecular string representations. *Patterns*, 3(10): 100588.
- Kusner, M. J.; Paige, B.; and Hernández-Lobato, J. M. 2017. Grammar Variational Autoencoder. arXiv:1703.01925.
- Landrum, G. 2016. RDKit: Open-Source Cheminformatics Software.
- Li, Y.; Vinyals, O.; Dyer, C.; Pascanu, R.; and Battaglia, P. 2018. Learning Deep Generative Models of Graphs. arXiv:1803.03324.
- Liu, Y.; Zhao, T.; Ju, W.; et al. 2017. Materials discovery and design using machine learning. *Journal of Materiomics*, 3(3): 159–177. High-throughput Experimental and Modeling Research toward Advanced Batteries.
- Perez, E.; Strub, F.; de Vries, H.; et al. 2018. FiLM: Visual Reasoning with a General Conditioning Layer. In *Proceedings of the Thirty-Second AAAI Conference on Artificial Intelligence and Thirtieth Innovative Applications of Artificial Intelligence Conference and Eighth AAAI Symposium on Educational Advances in Artificial Intelligence*. AAAI Press. ISBN 978-1-57735-800-8.
- Podda, M.; Bacciu, D.; and Micheli, A. 2020. A Deep Generative Model for Fragment-Based Molecule Generation. In *Proceedings of the Twenty Third International Conference on Artificial Intelligence and Statistics*, volume 108 of *Proceedings of Machine Learning Research*, 2240–2250. PMLR.
- Radford, A.; Kim, J. W.; Hallacy, C.; et al. 2021. Learning Transferable Visual Models From Natural Language Supervision. In *Proceedings of the 38th International Conference on Machine Learning*, volume 139 of *Proceedings of Machine Learning Research*, 8748–8763. PMLR.
- Ramakrishnan, R.; Dral, P. O.; Rupp, M.; and von Lilienfeld, O. A. 2014. Quantum chemistry structures and properties of 134 kilo molecules. *Scientific Data*, 1(1).
- Reddi, S. J.; Kale, S.; and Kumar, S. 2018. On the Convergence of Adam and Beyond. In *ICLR*.
- Runcie, N. T.; and Mey, A. S. 2023. SILVR: Guided Diffusion for Molecule Generation. *Journal of Chemical Information and Modeling*, 63(19): 5996–6005.
- Saharia, C.; Chan, W.; Saxena, S.; et al. 2022. Photorealistic Text-to-Image Diffusion Models with Deep Language Understanding. In *Advances in Neural Information Processing Systems*, volume 35, 36479–36494. Curran Associates, Inc.
- Sousa, T.; Correia, J.; Pereira, V.; and Rocha, M. 2021. Generative Deep Learning for Targeted Compound Design. *Journal of Chemical Information and Modeling*, 61(11): 5343–5361.
- Tang, Z.; Gu, S.; Bao, J.; et al. 2023. Improved Vector Quantized Diffusion Models. arXiv:2205.16007.

Turney, J. M.; Simmonett, A. C.; Parrish, R. M.; et al. 2012. Psi4: an open-source ab initio electronic structure program. *WIREs Computational Molecular Science*, 2(4): 556–565.

Vignac, C.; Krawczuk, I.; Siraudin, A.; et al. 2023. DiGress: Discrete Denoising diffusion for graph generation. In *ICLR*.

Weininger, D. 1988. SMILES, a chemical language and information system. 1. Introduction to methodology and encoding rules. *Journal of Chemical Information and Computer Sciences*, 28(1): 31–36.

You, J.; Liu, B.; Ying, Z.; et al. 2018a. Graph Convolutional Policy Network for Goal-Directed Molecular Graph Generation. In *Advances in Neural Information Processing Systems*, volume 31. Curran Associates, Inc.

You, J.; Ying, R.; Ren, X.; et al. 2018b. GraphRNN: Generating Realistic Graphs with Deep Auto-regressive Models. In *Proceedings of the 35th International Conference on Machine Learning*, volume 80 of *Proceedings of Machine Learning Research*, 5708–5717. PMLR.